Simulation based study of battery electric vehicle performance in real world cycles

Aditya Dhand and Keith Pullen

School of Engineering and Mathematical Sciences

City University London

London EC1V 0HB, UK

Email: aditya.dhand.1@city.ac.uk

Abstract

The development of battery electric vehicles (BEV) must continue since this offers the leading route towards a zero emission transport system. The fuel flexibility of the BEV offers the greatest potential to utilize power from renewable or low emission sources to be used in the transport system. However the limited range and high cost of the BEV remain important issues to be addressed. The battery is the element which strongly affects the cost and range of the BEV. The batteries offer either high specific power or high specific energy, but not both. This paper presents the modelling of a BEV which is used to study the potential for improvement in its energy efficiency. The battery model types have been discussed. The vehicle and other component models have been described. The choice of model parameters and the control strategy has been explained. The simulations have been performed on homologation and real world cycles for different scenarios. Results show significant potential for improvement in the energy efficiency of the BEV in real world usage by the utilization of a secondary energy storage device.

Keywords: battery, specific power, specific energy, battery model, vehicle simulation, drive cycle

Introduction

The battery electric vehicle has been operating on the road since the inception of the automobile. They were popular in the beginning of the 20th century as the internal combustion engine vehicles (ICEV) were less attractive at that stage. In 1900 out of the total sales of automobiles in the US about 38% were BEVs as compared to 22% ICEVs with steam powered vehicles making the rest of the numbers [1]. However with the rapid improvement in ICEVs, the BEVs started losing their popularity. By 1930s the BEV had almost disappeared from the scene. They gained impetus periodically in the last century such as during the 1973 oil crises but were always stuck at the prototype stage or were

produced in small numbers. The introduction of production hybrid electric vehicles (HEV) by Toyota in 1997 and subsequently by Honda in 1999 triggered a number of HEVs to be mass produced by other manufacturers in the 2000s. Since the last few years a small number of mass produced BEVs such as the Nissan Leaf, the Mitsubishi iMiEV and the Tesla Roadster have been introduced in the markets worldwide and many more are in the pipeline. However their cost and range are still issues that impede their popularity.

Baseline vehicle

The configuration of a modern BEV is shown in fig. 1.

The powertrain consists of an energy storage device which is a rechargeable battery in most cases powering one or more electric machines connected to the driveline. The electric machines might be connected to driveline directly as wheel hub machines or using a single speed or multi speed transmission. There is usually a power converter for AC/DC conversion as most BEV electric machines are AC machines. The primary energy source is usually a high voltage battery and the auxiliary power source is the standard 12 v battery. Most auxiliary loads are electric in nature unlike the conventional vehicle where they are mechanical. The BEVs also have an on board charger which is used to charge the high voltage battery. The vehicle controller and energy management system control the flow of energy. An inherent advantage of BEVs is that they can perform regenerative braking unlike conventional vehicles.

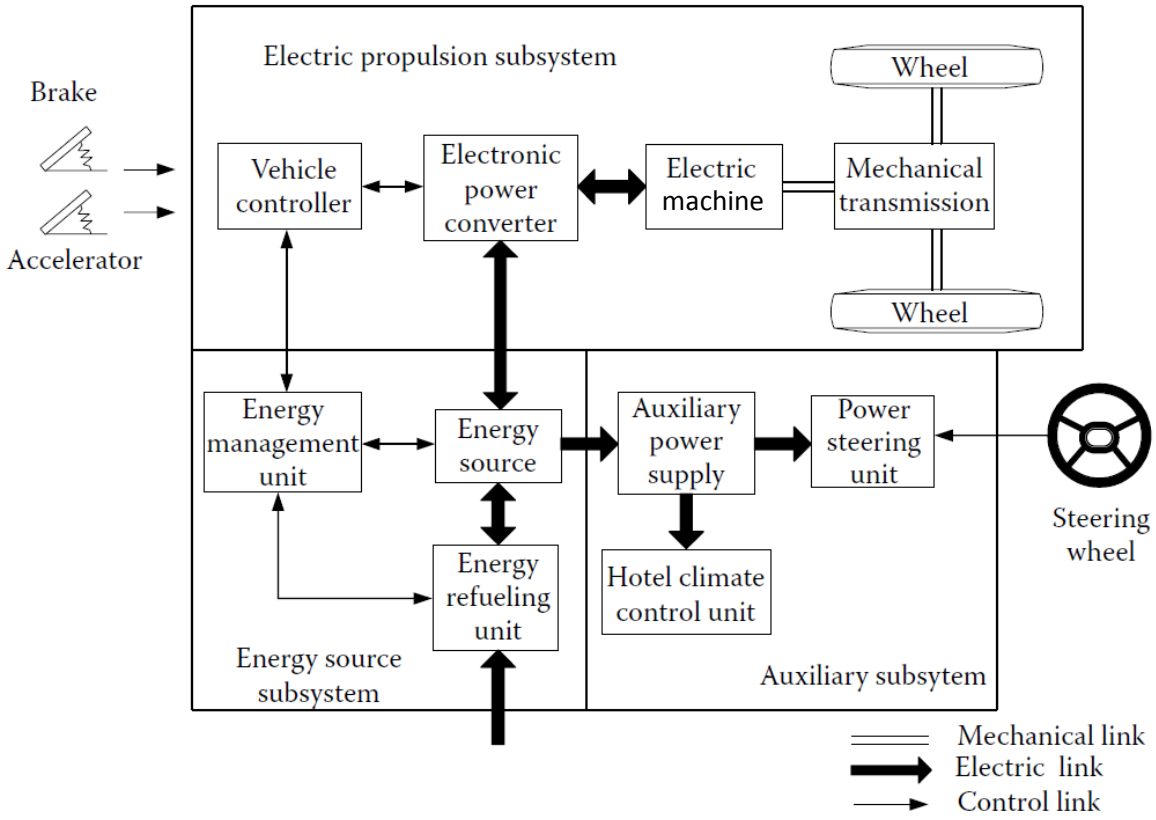

Figure 1: Schematic of BEV powertrain [2]

Battery

The most important element in the BEV is the battery. The battery in a BEV is constituted of a number of modules in series or parallel to achieve the desired voltage and current. The modules are in turn formed by connecting a number of cells in series or parallel. The cell is the smallest element of the battery. The general terminology related to batteries is given in [3].

As described by Ehsani et.al. (2010) and Chan et. al. (2001), there are different types of cell chemistries and the most popular for a modern BEV is the Lithium ion (Li-ion). However Li-ion is really a group of chemistries in which the anode is usually a lithium metal oxide and there are a variety of different compounds that can be used. Some of the important chemistries are described below [4]:

- Lithium iron phosphate (LFP)
- Lithium nickel manganese cobalt oxide (NMC)
- Lithium nickel cobalt aluminium (NCA)
- Lithium titanate oxide (LTO)
- Lithium manganese spinel oxide (LMO)

Some of the important properties of cells are specific energy, specific power, life cycle, safety and cost. Safety is linked to the thermal and chemical stability of the cell. The different chemistries have their different properties. LFP and LTO are considered to have high safety and life than Nickel-Cobalt chemistries but the latter usually have higher specific energy [5]. As with various technologies there are trade-offs. Another important aspect is the specific power which is usually a trade off with specific energy. As indicated by Burke et. al. (2009) any specific power can be achieved for all chemistries by sacrificing specific energy.

The following fig. 2 shows the Ragonne plot for various cell chemistries.

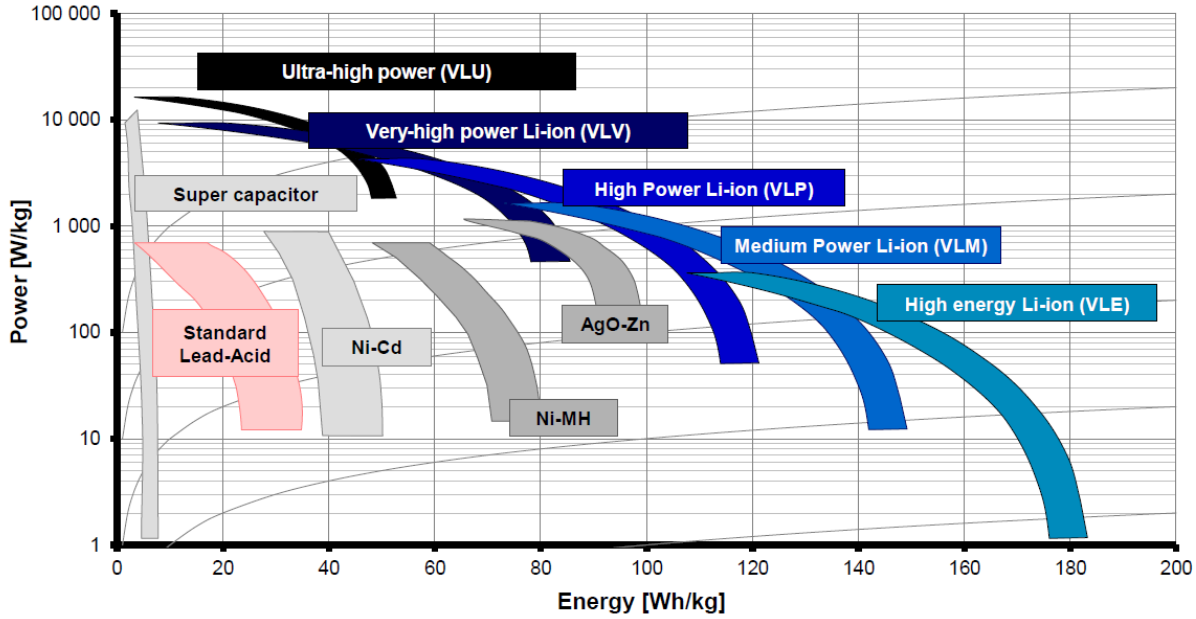

Figure 2: Ragonne plot for various battery chemistries [6]

From the fig. 2 it can be seen that the Li ion chemistry can be designed from very high power to high energy. The energy in very high power cells is about 35% the energy of high energy cells [7]. Usually for the BEV a high energy cell is more useful as compared to a HEV where high power is more essential. Not only is the chemistry of the cell important in deciding the properties, also the shape of the cell has significant effect in deciding the specific energy and specific power. Currently the cells are shaped into cylindrical, prismatic or pouch shapes which are shown in the fig. 3. The shape of the cell decides the surface area and volume of the cell. While for high power a bigger surface area is essential so that the lithium ions can be ionized in the electrolyte, transferred from one electrode and intercalated into another, a high energy cell requires a higher volume to store more charge [4]. It can therefore be said that the surface area to volume ratio of the cell is a significant parameter for design. A cell with thin electrodes will provide for bigger surface area whereas a thicker electrode will provide more volume. As the resistance of the cell is inversely proportional to the surface area and directly proportional to the thickness, the high energy cells have higher internal resistance than high power cell and consequently lower energy efficiency. The high energy cell will have higher power losses at high loads as compared to high power cells.

Figure 3: Cell designs (Cylindrical, Prismatic and Pouch) [4]

The cells are connected in series or parallel to create battery packs for BEV. There can be either a large number of small cells or fewer large cells. According to Pesaran et. al. (2009) using smaller cells has the benefit of lower cost (commodity market), improved safety and high quality production but they suffer from higher integration costs, complicated assembly, a large number of interconnects, lower weight and volume efficiency, lower reliability and costly electrical management. The larger cells have the benefit of lower assembly cost, higher weight and volume efficiency, better reliability though they have higher cell cost, lower quality and difficult thermal management. These are design trade-offs which need to be considered for particular applications [8]. According to Cluzel et. al. (2012), the cell size in the range 40-60 Ah are of good quality currently [9]. They are appropriate for vehicle application.

Battery modelling

Modern batteries can be modelled in various ways and there are three main types of modelling techniques. The electrochemical model is one of the techniques which describe the dynamic process of chemical reactions occurring on the electrodes based on mathematical method, which can integrally reflect dynamic characteristics of the battery [10]. They consist of partial differential equations with a large number of unknown parameters and do require detailed understanding of the battery design. One such model is the Shepherd model which is a simplified electrochemical model [11].

Another type of battery model is the data driven neural network model [12]. In this case a data set is used for training the model to identify the non-linear battery characteristics during charging and discharging. However the disadvantage of this model is that it requires large amount of data for training and validation.

The third type and one of the more popular one is the equivalent circuit (EC) model. In this case the battery is modelled as a network of resistances and capacitances (RC) to characterize their non-linear behaviour. They usually consist of a voltage source connected with RC elements. The voltage source typically models the open circuit voltage of the battery whereas the rest of the elements model the internal resistance along with other dynamic effects such as polarization. The EC models

are accurate to predict the dynamic behaviour of the battery however they require precise experimental results to parameterize the model. Different authors have used different methodologies to build these models. Zhang et. al. (2009) use Extended Kalman Filter technique to parameterize the EC model whereas Rahmoun et. al. (2012) use non-linear least squares algorithm [13].

Among the EC models there are different types with varying complexity. The simplest one is the so called Rint model where there is an open circuit voltage (OCV) source connected in series with an internal resistance. The open circuit voltage and internal resistance can be specified as function of SOC, temperature and charging or discharging process. According to Rahmoun et. al. (2012), this model is not suitable for any dynamic operation as it does not represent the transient behaviour of Li-ion cells. Another type is the one RC model in which the Rint model is connected in series with a parallel RC network to model the transient behaviour of the cell. This is called the Thevnin model or One Time Constant model. This allows the modelling of one time constant for charging and discharging. Antaloae et. al. (2012) observe that Li ion cells exhibit a second longer time constant in practice which reduces the modelling error in longer discharge cycles [14]. This is modelled by adding another RC network to the Thevnin model and is called Dual Polarization model (DP) or Two Time Constant model. The fig. 4 below shows the circuit of the Rint, Thevnin and DP models. According to He et. al. (2012) and Rahmoun et. al. (2012), the dual polarization model is the most accurate one for dynamic operations. It is decided to use this type of model in the present analysis.

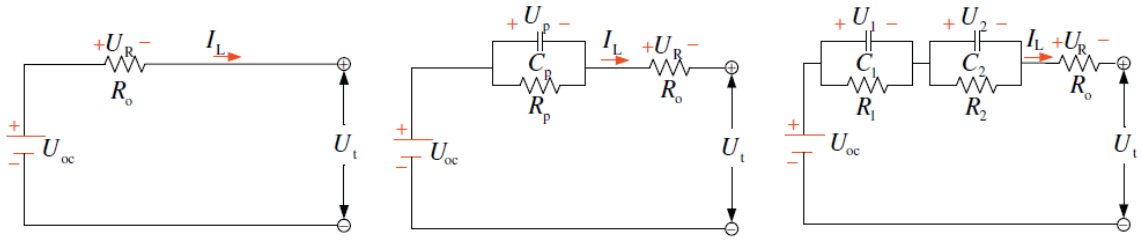

Figure 4: Battery models (Rint, Thevnin and DP) [11]

Another important aspect of battery model is the calculation of state of charge (SOC). The most common method is called coulomb counting where the current is integrated over time to calculate the SOC. For real life application in a battery monitoring system (BMS), this method can introduce errors due to uncertainty over the start SOC and the error can accumulate over time. Another method is the voltage based SOC correction which is again not suitable for BMS application. Other methods which treat the OCV as an internal variable and estimate SOC from the battery model have been developed which are suitable for BMS applications [15]. However for the present analysis the simple coulomb counting method is deemed sufficient as it is a comparative analysis using simulation.

Vehicle Model

The present analysis deals with the longitudinal dynamics of the vehicle and these are sufficiently and accurately represented by empirical map based models. This type of models can be constructed in Simulink like ADVISOR [16] or PSAT [17]. However there are commercial packages available such as AVL Cruise which can be used to construct them with relative ease [18]. The modular structure of AVL Cruise offers the flexibility in modelling and can perform a variety of tasks such as cycle run, full load performance and climbing performance. It offers the option of both forward and backward simulation and can be linked up with other tools such as Simulink which are more suitable for control system modelling. In the forward modelling approach a driver model is necessary which tries to control the vehicle via pedal movement to achieve the target vehicle velocity. However in the backward approach the calculation is done from wheel to the powertrain. The forward approach is more realistic though the backward approach is faster to run. For this analysis the forward approach is taken. The difference between forward and backward approach is explained in detail [19].

A C-segment passenger car is taken as the base vehicle for this study as this is the one of most common mode of private transport especially in Europe. The vehicle is a 5 door hatchback front wheel drive with a kerb weight of 1445 kg. The particulars of the vehicle are mentioned in the table 1.

Table 1: Vehicle parameters

Parameters	Value
Kerb mass	1445 kg
Gross mass	1884 kg
Frontal area	2.29 m^2
Drag coefficient	0.29
Wheel radius	301 mm
Rolling resistance	0.009

The two time constant model is preferred for the battery and the 3.7 V Li ion polymer cell modelled in [13] is used for this analysis. The specific energy of the cell is mentioned as 163 Wh/kg by the manufacturer which would classify it as a high energy cell suitable for BEV. It is taken to construct a pack of 98 cells in series giving a nominal voltage of 362.6 V for the vehicle. This would constitute a battery pack with capacity of 53 Ah and energy of 19.2 kWh, which is similar to the ones used in modern BEVs. The cell model parameters are mentioned at 25 deg C and that is taken as the working temperature of the pack. The peak pulse current discharge limit is 260 A. Some parameters such as mass of the cell are taken from the manufacturer's website [20]. The mass of the battery pack is modern BEVs is about double the total mass of the cells and similar assumption is used to constitute the battery pack mass for the base vehicle which amounts to be about 225 kg. The auxiliary loads are taken to be 300 W which is a reasonable assumption for the average power consumption related to power requirements for vehicle house-keeping. This does not include heating, ventilation and air-conditioning loads. This load is directly added to the electric machine load at the battery terminals.

The electric machine is a 72 kW machine which is scaled down from the 80 kW machine mentioned in [21] to match the peak power of the battery which is about 77 kW. The maximum torque performance and the efficiency of the machine, which includes the power inverter efficiency, in motoring mode are illustrated in [21] and the same is assumed for the generating mode. The rotating inertia of the original machine is estimated to be 0.0657 kgm^2 from its dimensions and mass. The scaled down EM has maximum power of 72 kW, maximum torque of 252 Nm and maximum speed of 10,390 rpm. The EM is connected to a single speed transmission of ratio 7.93, which has an efficiency of 98%. The characteristics of the machine are shown in fig. 5 and are assumed the same for all voltages. The map shows constant efficiency of 85% below 1000 rpm. It was extrapolated to create efficiency values below 1000 rpm at constant torque and was found that the effect of this change on cycle simulation results is marginal; therefore the efficiency below 1000 rpm was kept as the original 85%. The map based modelling approach is commonly used for the electric machine in BEVs [22].

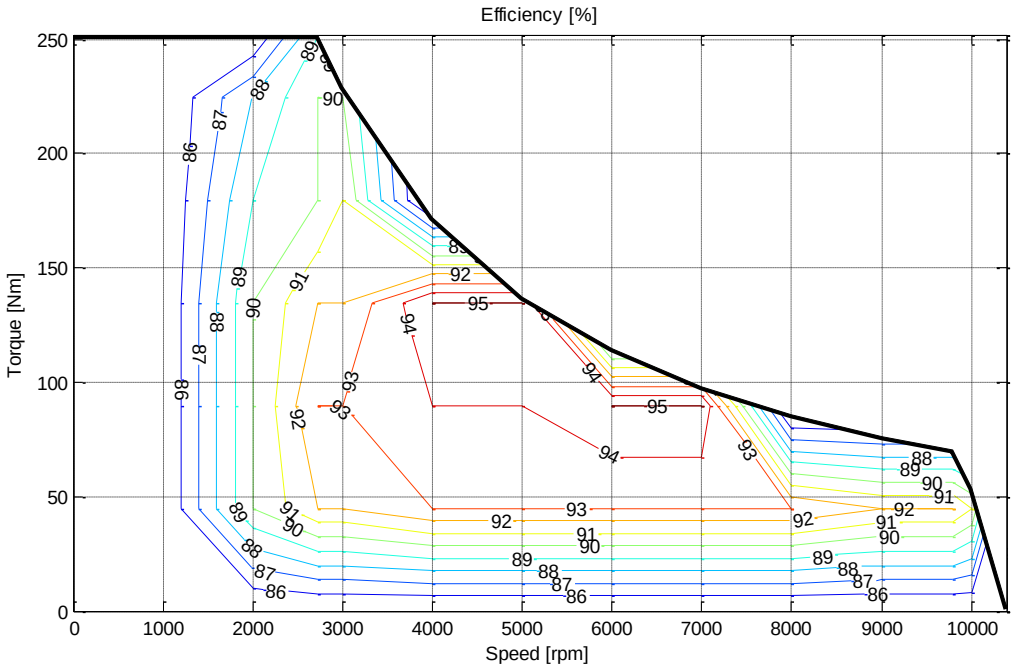

Figure 5: EM properties

There are two operating modes in the vehicle, namely motoring and braking. The motoring control is relatively straightforward. For motoring purposes the driver controls the accelerator pedal to match the desired vehicle speed and that is converted to the load signal for the electric machine which powers the vehicle forward. The braking mode requires a strategy different from the conventional vehicles since there is possibility of regenerative braking. The regenerative braking strategy used is similar to the one mentioned in [23]. The required braking torque is calculated from the brake pressure signal which comes from the brake pedal controlled by the driver to achieve the desired deceleration. This brake torque is compared to the available electric machine generating torque and the brake torque limit of the front axle. The minimum of the three values is taken as the desired electric machine torque which is converted into the load signal for the electric machine. If at all the brake torque requested by the driver is higher than the available EM torque, the rest is provided by the mechanical braking.

In AVL Cruise the brake pressure signal is same for all the four brakes and the brake size for the front and rear brakes, is dependent on the mass distribution of the vehicle. In this case an equal mass distribution for the front and rear axle is assumed. This is a reasonable assumption as the heavy batteries are usually in the rear of the vehicle. The dimensions of the brake are used to compute the brake torque according to the following equation. The model takes into account the change in axle load due to acceleration or deceleration. This front axle load which is a model output, is used to compute the front axle load limit. According to most standard driving cycles, the maximum deceleration is about 0.4g which is easily achievable by braking only the front axle if the standard road conditions, which have an average friction coefficient of 0.8-0.9 [2], are assumed. It can be seen in the fig. 6, that the maximum brake force demand for various drive cycles which is calculated by using the maximum deceleration rate and neglecting the resistance force, is lower than the front axle brake limit calculated under steady state conditions, for all drive cycles except HYZEM road cycle.

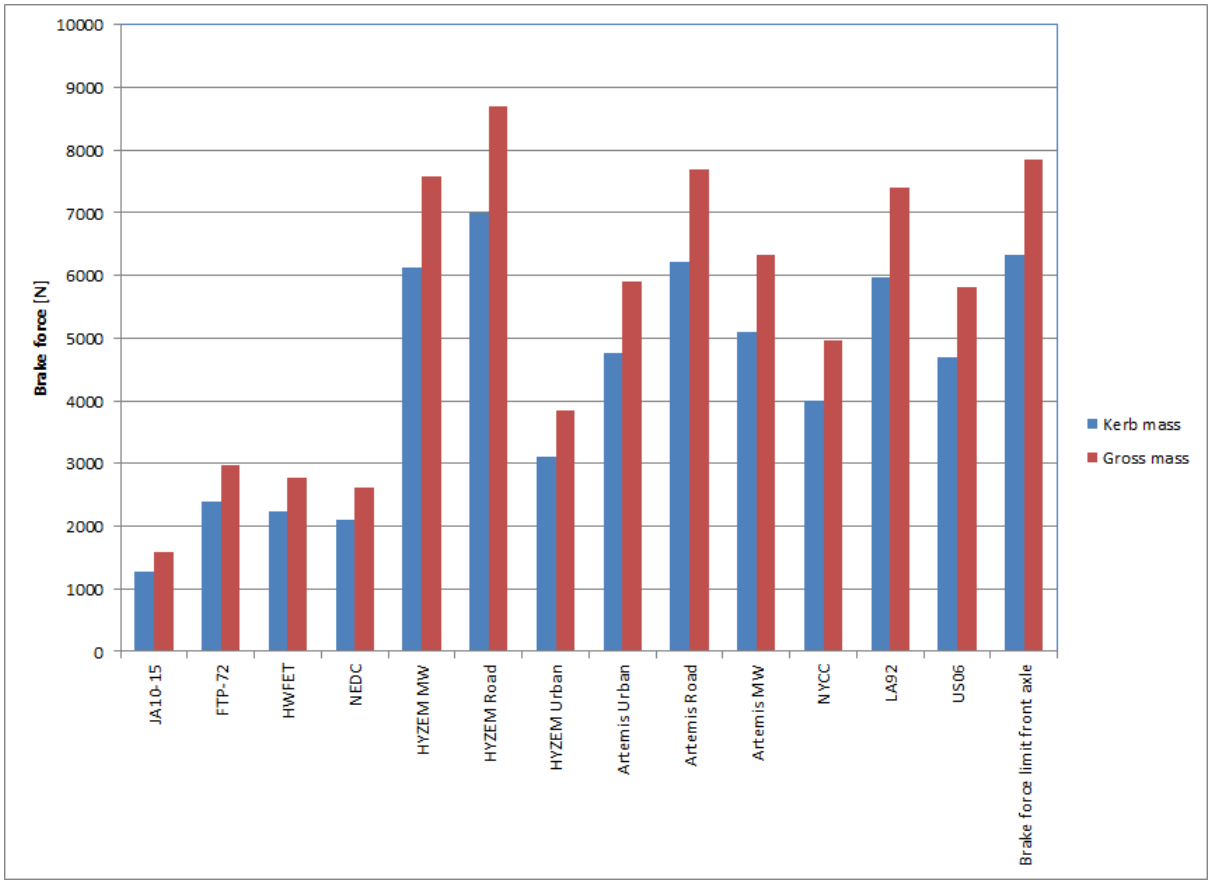

Figure 6: Brake force

With regenerative braking a few more conditions have to be incorporated to protect the EM and the battery. It is not easy for the electric machine to generate electricity at low vehicle speed which implies low EM speed, because of the very low electric motive force (voltage) generated at that speed [23]. Therefore the EM is not used for regenerative braking below 10 kph. Another factor is the battery SOC. At close to full SOC the battery is protected from over charging by limiting regenerative braking and to include this effect in the present analysis the regenerative braking is only allowed below 90% SOC. Fig. 7 shows the model schematic in AVL Cruise.

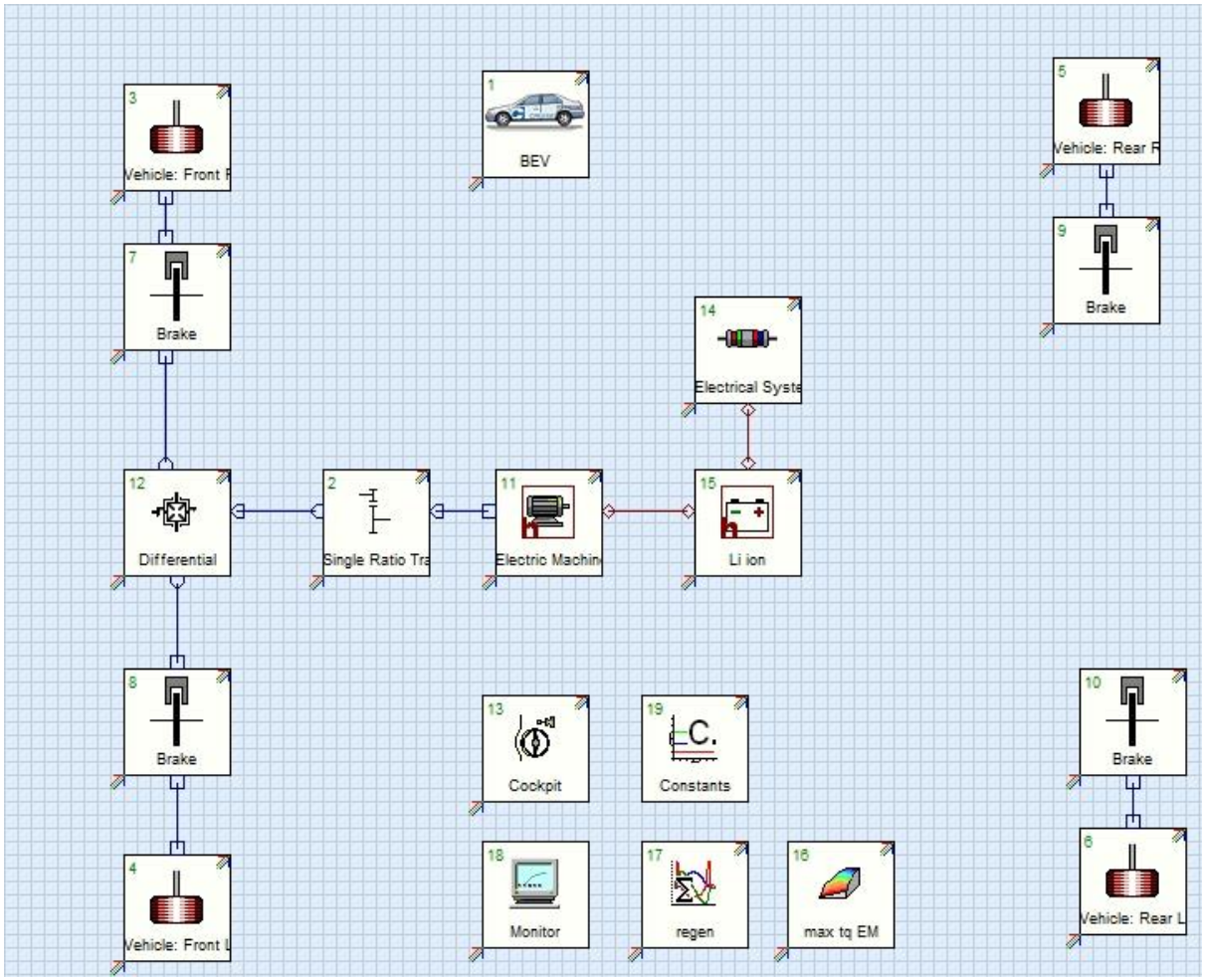

Figure 7: Vehicle model

Drive cycle simulation

The standard homologation drive cycles which are used for the fuel consumption simulation include the New European Drive Cycle (NEDC), Federal Test Procedure (FTP-75), Highway Fuel Economy Test (HWFET) and the Japanese 10-15 drive cycle. As mentioned before the simulations are carried out in the forward simulation mode and at steady state temperature of 25 deg C. The wheel slip is not considered. The maximum simulation time step is taken to be 10 ms which gives sufficient accuracy. The vehicle test weight during the simulations is taken as the kerb mass plus an additional mass of 75 kg to simulate the driver. The simulations are carried out at initial SOC of 100% and 90% to show the benefit by regenerative braking. Table 2 shows the result of the simulation.

From the table 2 the effect of regenerative braking can be easily seen in the energy consumption figures. Considerable improvement is seen in all the cycles where the energy consumption reduces by 23-34% with regenerative braking, except HWFET. The lowest benefit of only 5% is seen in HWFET since it is highway cycle with limited opportunity for regenerative braking.

Another important parameter which is calculated for the cycles is the cycle round trip (RT) battery efficiency. One of the model outputs is the power loss in the battery primarily due to its internal resistance and other factors such as polarization. Integrating this power loss over the cycle time gives the energy lost in the battery and with the net energy output at the battery terminals known, the round trip battery efficiency is calculated by taking ratio of net energy output to the sum of net energy output and energy lost. It can be seen from the table that the battery gives round trip efficiency of about 90% or more on all the standard drive cycles.

Table 2 Results for Homologation Drive Cycles

	Energy consumed at battery terminals [kWh/km]		Improvement in Energy consumed [%]	Battery Round trip Efficiency [%]
	Start SOC 100%	Start SOC 90%		Start SOC 90%
NEDC	0.1409	0.1083	23.1	90.9
FTP-72	0.1454	0.0963	33.7	89.7
JA1015	0.1438	0.0947	34.1	92.3
HWFET	0.1210	0.1148	5.1	93.9

Real world driving cycles

A problem with the homologation cycles mentioned in the previous section is that they do not represent the real world driving situation. They are made for testing vehicles on the chassis dynamometer and have lower acceleration and deceleration rates than what is encountered in real world driving. This is done to make the testing easier to perform. However in the last 10-15 years a lot of work has been done to create real world driving cycles such as Artemis cycles [24] and Hyzem cycles [25]. Other real world cycles such as US06, LA92 and New York City Cycle (NYCC) have also been created. The US06 is an aggressive highway driving cycle, the LA92 represents the extra-urban driving conditions in California and NYCC represents the urban driving condition in New York. The fig. 8 shows the average velocity and root mean square (RMS) acceleration behaviour for these driving cycles.

In the fig. 8, the results of a statistical analysis of cycles show that the homologation cycles have much lower acceleration than the real world cycles. The US06, LA92 and Artemis urban cycles seem to have the highest acceleration over the entire speed range. Only the Artemis and Hyzem motorway cycles seem to have higher average velocities than the rest of the cycles. For the present analysis the US06, LA92 and Artemis urban cycles are taken as reference for the real world cycle usage.

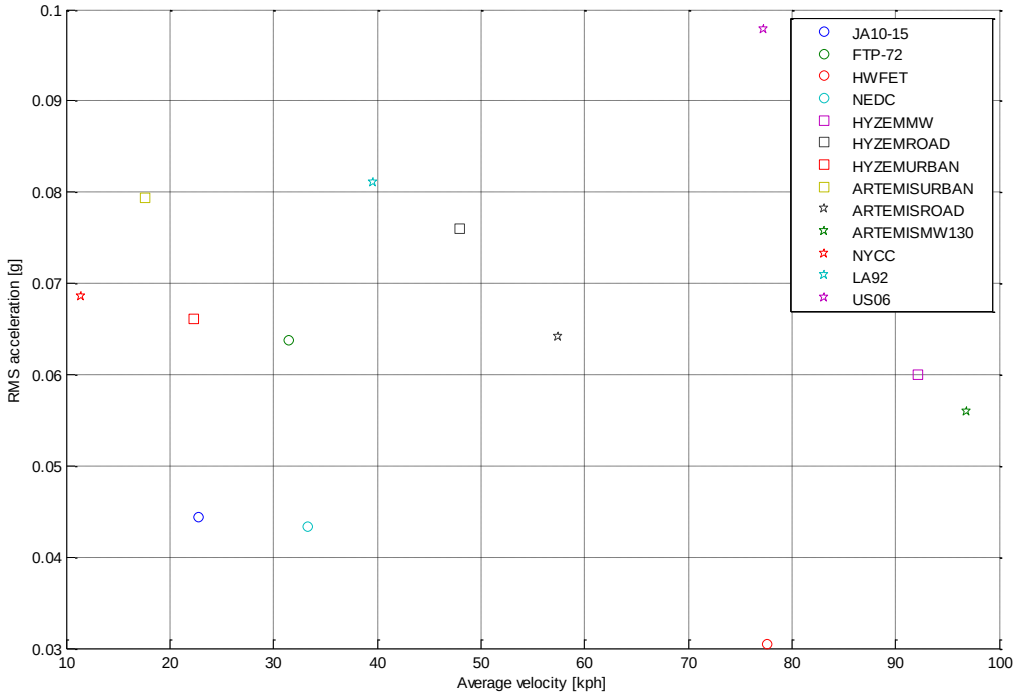

Figure 8: Drive cycle properties

Table 3 shows the results of vehicle energy consumption for the US06, LA92 and Artemis urban cycle with start SOC 90%. As can be seen the energy consumption under these cycles is higher than most of the homologation cycles though the interesting result is the overall cycle round trip battery efficiency which is significantly lower than for the homologation cycles. It can be seen that the roundtrip battery efficiency in these real world cycles varies from 78-83% as compared to at least 90 % for the homologation cycles. The worst case is the US06 cycle where it is about 78%. Fig. 9 shows the trend comparing RMS acceleration of cycles vs. battery round trip efficiency. It can be broadly seen that as the RMS acceleration increases the efficiency goes down, hence there is a reasonably good correlation. It is expected that in more demanding terrain such as hills the efficiency could be further reduced.

Table 3: Real world drive cycles

	Energy consumed at battery terminals at start SOC 90% [kWh/km]	Battery Round trip Efficiency [%]
US06	0.1546	78.6
LA92	0.1167	82.4
Artemis Urban	0.1100	83.6

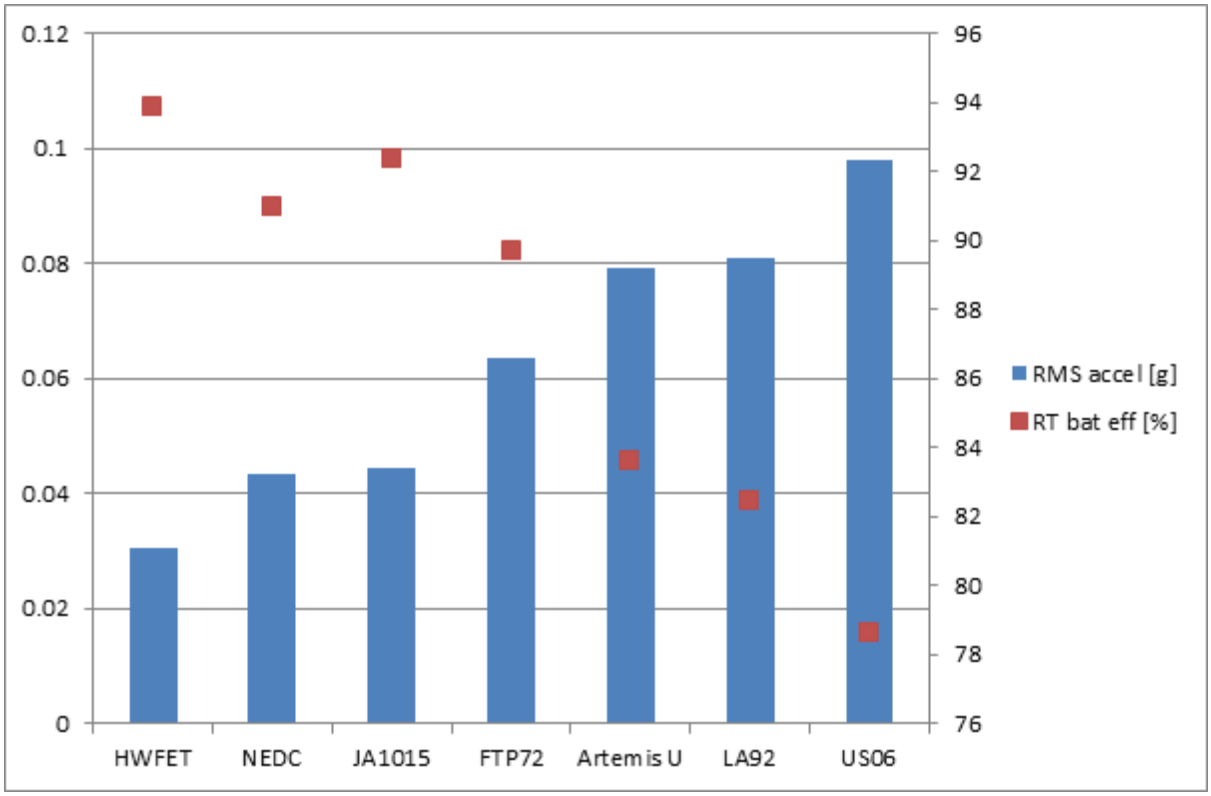

Figure 9: RMS acceleration vs. RT Battery efficiency

The average power consumed during these cycles is calculated by dividing the net energy consumed at the battery terminals by the cycle duration. The next table 4 shows the average power consumed during these drive cycles and the simulation results when the battery load is fixed to the average power for the duration of the cycle. The peak power is many times the average power and the worst case is the Artemis urban cycle where it is almost 24 times the average power. However when the average power is applied to the battery for the duration of the cycle, the net energy output from the battery terminals is the same as before but the difference is in the cycle roundtrip battery efficiency which is more than 96% for all the cycles. It is more than 99% for the Artemis urban cycle and 96.2% for the US06 cycle. Thus it can be seen that the power losses inside the battery can be theoretically reduced significantly if a low constant load is applied instead of the actual dynamic load. This presents a possibility for improving the energy efficiency by utilizing a secondary storage device for power handling.

Table 4: Average power results

	Average Power [kW]	Ratio of peak to average power	Battery round trip efficiency with average power [%]
US06	11.95	5.95	96.2
LA92	4.62	14.7	98.6
Artemis Urban	1.94	23.8	99.4

Another result to observe is the powertrain efficiency which is defined as the ratio of the power at the wheels to the power output of the battery during motoring and reverse during regenerative braking. The powertrain efficiency during motoring is calculated for the cycle by integrating the traction power at the wheels during motoring and dividing that by the energy output from the battery terminals. Similarly the powertrain efficiency during brake regeneration is calculated by taking the energy input at the battery terminals and dividing it by the integral of the brake power demand at the wheels during brake regeneration. The results show that in cycles with low average speed and low RMS acceleration the positive and negative powertrain efficiencies are lower. Fig. 10 shows the positive powertrain efficiency for various cycles (bubble size represents RMS acceleration [g]).

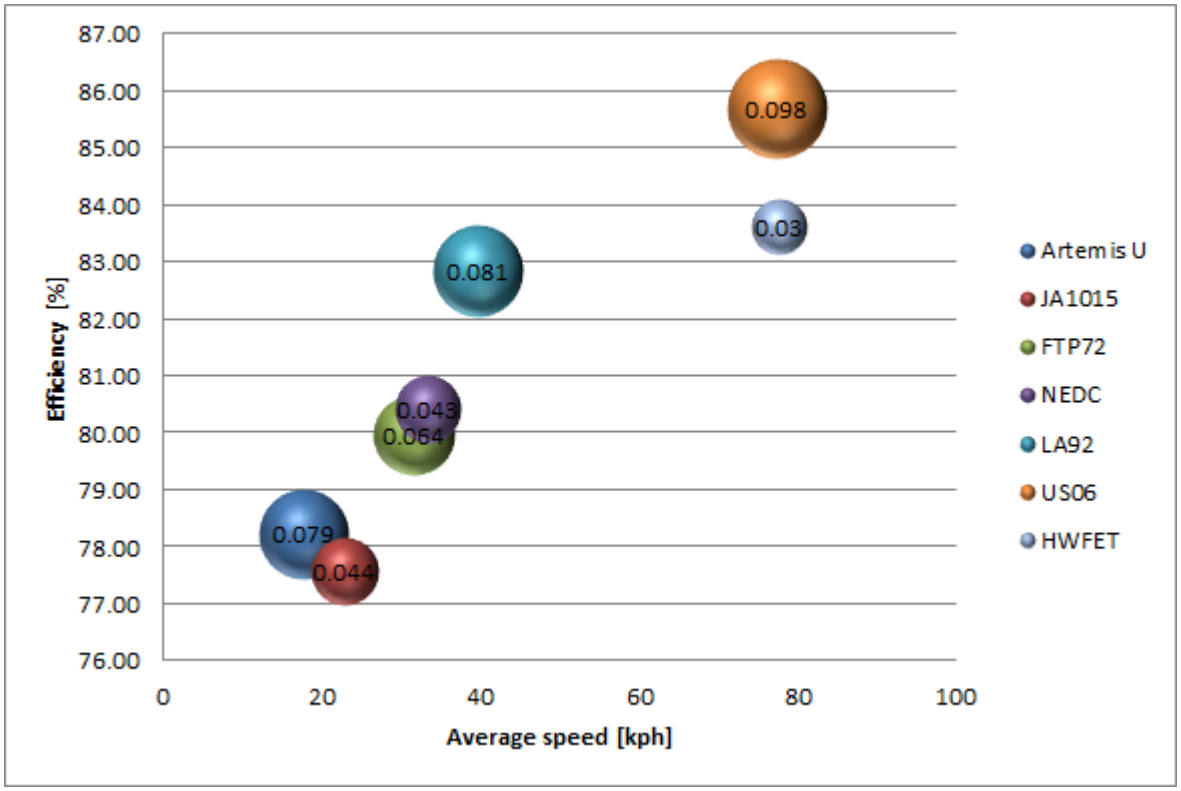

Figure 10: Powertrain Efficiency

In the very low average speed cycles such as JA1015 and Artemis Urban, the efficiency seems to be impacted little by average speed and RMS acceleration values. However, in the lower average speed region, say up to 30 kph, the powertrain efficiencies seem to be impacted less by RMS acceleration and more impacted by average speed e.g. in case of JA1015 and NEDC. In the high average speed region, the powertrain efficiencies are affected by RMS acceleration though the impact is smaller e.g. in case of US06 and HWFET. The reason for the higher efficiency values is apparent from the EM efficiency map, which is the major contributor towards powertrain efficiency, where the higher

efficiency is observed towards the maximum power region and at lower speeds especially below 1000 rpm the efficiency is relatively low (around 85%) and independent of torque.

The following figures show the time weighted operating points of a drive cycle plotted over the efficiency map of the EM [26] (the bubbles represent the operating points with their size representing their residency in the cycle). It can be seen in the fig 11 that for Artemis urban cycle, nearly 50% of the time, the EM operates in the below 1000 rpm speed region and in that region the efficiency is independent of torque. In the higher speed region, they operate in low torque regions and that part of the operation might be benefited by downsized EM.

Looking at the similar figs. 12 and 13 for LA92 and US06 cycle it is clearly seen that the more points are operating in the higher efficiency regions and higher speed regions as compared to Artemis urban cycle. The higher speed points would benefit from a downsized machine as that would push the high speed and low torque points in the higher efficiency zones. Of course the US06 cycle has more points in the high efficiency region than the LA92. Thus utilizing a power handling device, which is able to transmit power to the driveline directly, would allow the downsizing the main electric machine. One such device is a flywheel with a mechanical continuously variable transmission (CVT).

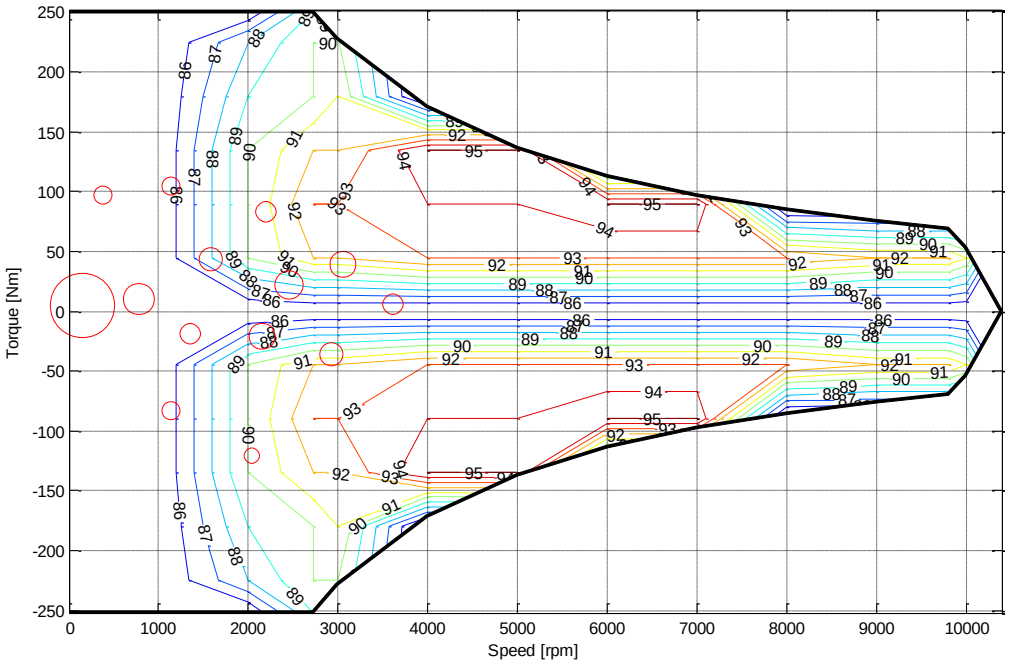

Figure 11: Artemis Urban operating points

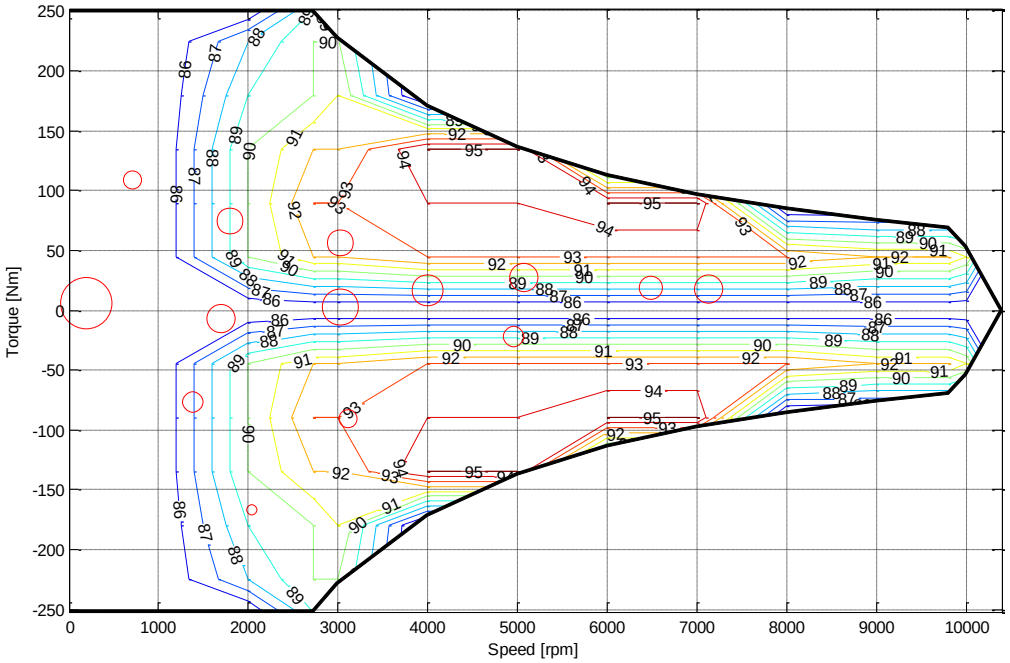

Figure 12: LA92 operating points

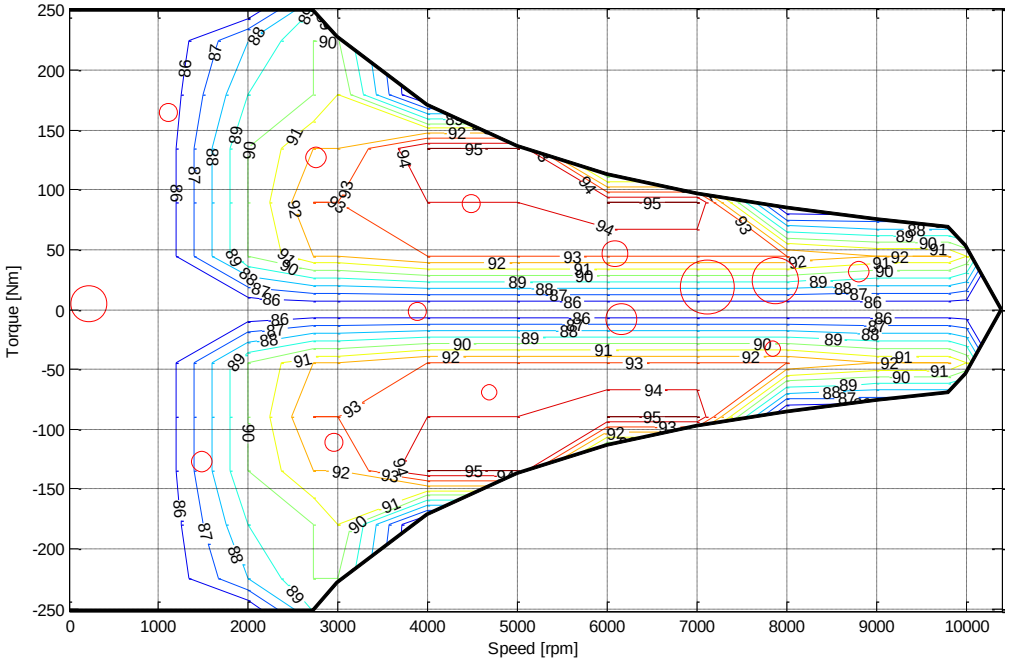

Figure 13: US06 operating points

Conclusions

The BEV is an important option to reduce the dependence on fossil fuels though it still has significant challenges in terms of cost and range. The Li ion batteries are significant improvement over the NiMH and lead acid batteries but they still are not sufficiently advanced to provide a satisfactory range. This paper presents the modelling of a BEV which is used to explore the potential in improvement of its energy efficiency. The model parameters and elements are described and the drive cycle simulation results are shown. The simulation results show that the high energy battery in the BEV performs well during homologation drive cycles but shows significantly lower round trip efficiency during real world cycles. The theoretical improvement in round trip efficiency is shown when the average load is applied to these cycles as compared to the actual dynamic load. The powertrain efficiency of the BEV is also explored and results show potential benefit could be achieved by downsizing the main prime mover. This presents the possibility of employing a power handling device, which could transmit power directly to the driveshaft, to improve the energy efficiency of the BEV. This would be explored in future work.

References

1. Chan, C. et. al., Modern Electric Vehicle Technology, Oxford University Press, 2001
2. Ehsani, M. et. al., Modern Electric, Hybrid Electric, and Fuel Cell Vehicles, Fundamentals, Theory, and Design, Second edition, CRC Press, Taylor & Francis Group, 2010
3. A Guide to Understanding Battery Specifications, MIT Electric Vehicle Team, December 2008
4. Omar, N. et. al., Rechargeable Energy Storage Systems for Plug-in Hybrid Electric Vehicles—Assessment of Electrical Characteristics, Energies 2012, 5, 2952-2988
5. Burke, A. et. al., Performance Characteristics of Lithium-ion Batteries of Various Chemistries for Plug-in Hybrid Vehicles, EVS24, Stavanger, Norway, May 13 - 16, 2009
6. De Guibert, A., Lithium batteries technologies for transportation applications, Keynote address, International scientific conference on hybrid and electric vehicles, RHEVE 2011
7. Miller, J., Energy storage system technology challenges facing strong hybrid, plug-in and battery electric vehicles, IEEE Vehicle Power and Propulsion Conference, 2009
8. Pesaran, A. et. al., Integration Issues of Cells into Battery Packs for Plug-in and Hybrid Electric Vehicles, EVS24, Stavanger, Norway, May 13 - 16, 2009
9. Cluzel, C. et. al., Cost and performance of EV batteries, Final report for The Committee on Climate Change 21/03/2012
10. Zhang, C. et. al. Identification of Dynamic Model Parameters for Lithium-Ion Batteries used in Hybrid Electric Vehicles, International Symposium on Electric Vehicles (ISEV), Beijing, China, September 2009
11. He, H. et. al., Comparison study on the battery models used for the energy management of batteries in electric vehicles, Energy Conversion and Management, Vol. 64, December 2012, 113–121
12. Singh, P. et. al., Fuzzy Logic Modeling of Unmanned Surface Vehicle (USV) Hybrid Power System, Proceedings of the 13th International Conference on Intelligent Systems Application to Power Systems, 2005

13. Rahmoun, A. et. al., Modelling of Li-ion batteries using equivalent circuit diagrams, Przegląd Elektrotechniczny (Electrical Review), R. 88 NR 7b/2012
14. Antaloae, C. et. al., A Novel Method for the Parameterization of a Li-Ion Cell Model for EV/HEV Control Applications, IEEE Transactions on Vehicular Technology, Vol. 61, No. 9, November 2012
15. Tang, X. et. al., Li-ion Battery Parameter Estimation for State of Charge, 2011 American Control Conference, San Francisco, CA, USA, June 29 - July 01, 2011
16. NREL, ADVISOR 2002, National Renewable Energy Laboratory: Golden, Colorado, USA
17. ANL, PSAT 2002, Argonne National Laboratory
18. AVL Cruise 2012, www.avl.com
19. Van Mierlo, J. et. al., Simulation methodologies for innovative vehicle drive systems, International power electronics and motion control conference, Riga, September 2004
20. Kokam Co. Ltd., www.kokam.com, accessed 15.12.2012
21. Sato, Y. et. al., Development of High Response Motor and Inverter System for the Nissan LEAF Electric Vehicle, SAE 2011-01-0350, 2011
22. Hofman, T. et. al., Energy Efficiency Analysis and Comparison of Transmission Technologies for an Electric Vehicle, IEEE Vehicle Power and Propulsion Conference, 2010
23. Guo, J. et. al., Regenerative Braking Strategy for Electric Vehicles, IEEE Intelligent Vehicles Symposium, 2009
24. Andre, M., The ARTEMIS European driving cycles for measuring car pollutant emissions, Science of the Total Environment, 334–335, 2004, 73–84
25. Andre, M., European Development of Hybrid Technology approaching efficient Zero Emission Mobility (HYZEM): Driving patterns analysis and driving cycles, INRETS Report LEN No 9709, July 1997
26. AVL Cruise version 2010, Condensation Description, Edition 11/2010